Relaxation Mössbauer spectra under rf magnetic field excitation

A. M. Afanas'ev
Institute of Physics and Technology, Russian Academy of Sciences, Krasikova 2a, 117218 Moscow, Russia

M. A. Chuev
Russian Research Center ''Kurchatov Institute,'' Kurchatov Square, 123182 Moscow, Russia

J. Hesse
Institut für Metallphysik und Nukleare Festkörperphysik, Technische Universität Braunschweig, Mendelssohnstrasse 3, D-38106 Braunschweig, Germany

(Received 2 December 1996)

In the present study the general equations which describe the absorption Mössbauer spectra under radio-frequency (rf) magnetic field excitation with arbitrary frequency and field strength have been derived. Within our model chosen for a ferromagnet as a system of exchange-coupled (interacting) Stoner-Wohlfarth particles, the evolution of the magnetization and the corresponding Mössbauer spectra as a function of temperature and initial magnetization relaxation parameters are traced. It is found that the collapse effect is of a pronounced threshold character with respect to the rf field strength and does not need strong rf fields for its realization. The necessary condition for the observation of a collapse effect is only a rf amplitude causing the corresponding magnetization curves to be symmetrical in time reversal. The theory developed allows us to perform calculations of Mössbauer spectra under rf magnetic field excitation and the corresponding magnetization curves (also for multiphase systems such as modern nanostructured magnetic alloys). The results are also useful in a situation when the hyperfine field at the nuclei does not follow the rf magnetic field. This circumstance determines the rather nontrivial transition from the collapsed line (in strong enough rf field) to the well-resolved hyperfine structure (in weak rf field) and contributes therefore in understanding the selective partial collapse effect. [S0163-1829(97)02033-X]

I. INTRODUCTION

More than 20 years ago, Pfeiffer[1,2] presented ^{57}Fe Mössbauer transmission experiments exposing a Permalloy absorber to radio frequency (rf) magnetic fields, in which the rf collapse effect has been observed. The well-resolved magnetically split spectrum was found to collapse in a strong enough rf field to a single central line of nearly natural linewidth. Later, this effect was often observed in other soft magnetic materials.[3–8] In recent time, the phenomenon has become of special interest due to the high efficiency of Mössbauer spectroscopy with rf excitation in the study of modern nanocrystalline magnetic alloys[9–11] and with the discovery of the partial selective collapse effect.[10] Pfeiffer suggested a simple physical explanation of the effect. The magnetization of the sample that exhibits soft enough magnetic properties will be switched in the direction following the external magnetic rf field. Because the hyperfine field vector at the nuclei is strongly coupled to the magnetic moments of the atoms, it also starts to change its direction in response to the rf field, so that it is always antialigned (at iron nuclei) with the applied field. Suppose that (i) the rf-field frequency is higher than the Larmor frequency of the nuclei in their hyperfine field and (ii) the rf-field amplitude is strong enough to drive the magnetization into saturation. In this case the magnetic hyperfine field at the nucleus will be averaged to zero and a single line (or a quadrupole doublet) pattern is expected to appear in the spectrum.

Along with the collapsed spectrum symmetric pairs of sidebands located at $\pm n\omega_{\mathrm{rf}}$ (ω_{rf} is the rf-field frequency) observed in Ref. 1, similar sidebands in the absence of the collapse effect were observed earlier in Mössbauer spectra[12,13] and treated as acoustically modulated sidebands due to the magnetostriction in the sample. Pfeiffer also associated the appearance of sidebands only with magnetostriction effects and even considered the fact of their appearance along with the collapsed line as evidence for the temperature of the sample under investigation being below the Curie temperature, which eliminates the appearance of the collapsed line due to rf sample heating above the Curie temperature point. In the following experimental studies of the collapse effect, a broadened collapsed line with no visible sidebands was observed at definite conditions.[5,6] The latter made the hypothesis of the magnetostriction origin of sidebands more reliable. However, the following theoretical works showed that the reversal of the sample's magnetization should necessarily result also in the appearance of sidebands even when magnetostriction vanishes.[14–16] The sideband appearance is due to the formation of energy quasilevels in the nuclear Zeeman subsystem under a fluctuating hyperfine field.[17] As a result, up to now the mechanism of sideband formation in the presence of the collapse effect remains open to some extent.

The rf collapse effect is revealed in clear form only in rf fields strong enough. In weak or intermediate fields, a very rich and complex picture of the transformation of Mössbauer spectra is observed.[4–11] However, up to now there is no theory that describes the transformation of Mössbauer spectra under excitation by rf fields of arbitrary strength even in a

simplified manner. The theoretical works mentioned above, already in their basis, were motivated to describe the absorption Mössbauer spectra only in the limiting case of strong rf field and were founded completely on the criteria proposed by Pfeiffer for the explanation of the collapse effect. Experimental spectra influenced by weak rf fields were not analyzed at all and often not cited.

The present work is just dedicated to the development of a theory describing absorption Mössbauer spectra under excitation of the sample by a rf field of arbitrary strength. The theory is based on the assumption of a stochastic nature of the time evolution of the hyperfine field $H_{\rm hf}(t)$. The magnetic dynamics of a system does not strictly prescribe the time dependence of $H_{\rm hf}(t)$, but defines only stochastic parameters of the time trajectories of $H_{\rm hf}(t)$. The complete set of expressions for absorption Mössbauer spectra can be derived for rf fields of arbitrary frequency and strength. For the case of strong rf fields, the expressions make the ''deterministic'' description of $H_{\rm hf}(t)$ be possible, and the known results for absorption spectra are derived.[16] The theory needs some clearly defined model to describe the magnetic dynamics of the system due to both thermal fluctuations and rf-field excitation. First of all, we will follow the ideas of Stoner and Wohlfarth[18] and consider a ferromagnet as an ensemble of single-domain particles (or clusters). Between the particles we assume an interaction which can be of exchange and/or dipole-dipole type. Further, we assume that the exchange interaction within a single particle exceeds the exchange and/or dipole-dipole interactions between the particles. The magnetic relaxation parameters of the system are evaluated in the framework of the molecular-field approximation. Their results are used to perform a calculation of the sample's magnetization and in the development of the theory describing the Mössbauer spectra under rf magnetic fields. This model seems to be the most appropriate for the ensembles of superparamagnetic particles[19,20] and magnetic alloys consisting of nanocrystalline and amorphous phases.[9–11] It also leads to a deeper understanding what the partial selective collapse effect is. Recently[10] it was experimentally found that in nanostructured ferromagnetic alloys the collapse effect is able to distinguish between the different phases. It appears only partially at the selective location of the nanograins.

First of all, this closed model establishes the criteria needed for observation of the collapse effect. Pfeiffer's criteria are sufficient to observe the collapse effect; however, in reality the effect can be found at less stringent limitations. It is found that the transition from the collapsed line to the visually resolved hyperfine structure occurs in a very narrow interval of the rf-field strength around h_a and is accompanied by qualitative changes in the magnetization-reversal process. The magnetic hysteresis curves above and below this transition point h_a are absolutely different in character: At $h > h_a$ the hysteresis curve is symmetrical for rf-field reversal, and at $h < h_a$ there is no such symmetry, but there exist two hysteresis curves transformed one into another with time reversal.

In Sec. III, a general equation for absorption spectra is derived. Even in its final representation, it appears to be rather complicated. The spectra are represented as a double integral over operator functions, and the operators are evaluated by means of the solution of nonlinear equations, the number of which may be rather great for systems with a number of phases and distributions of parameters of particles. Nevertheless, the calculation of the Mössbauer spectra can be performed using a normal PC for systems in which the number of parameters exceeds one hundred. In the limiting case of fast relaxation, symplified equations for absorption Mössbauer spectra are derived. In order to clarify the qualitative behavior of Mössbauer spectra under rf-field excitation, we will assume that the forced magnetostriction vanishes completely.

II. FOUNDATION OF THE PROBLEM

In magnetic materials subjected to a time-dependent magnetic field (i.e., rf field), complicated relaxation processes occur, which manifest themselves macroscopically, for instance, as a magnetization reversal with pronounced hysteresis behavior. The same processes influence absorption Mössbauer spectra. The shape of the spectra reflects more detailed information about the magnetic relaxation processes than magnetization measurements do. It is obvious that the magnetization reversal cannot be homogeneous over the sample's bulk because of the anisotropy energy and is going on in steps through particular small pieces if the latter are predetermined somehow by peculiarities of preparation and structure of the magnetic material as well as by exchange interactions. The most striking example here is a system of superparamagnetic particles, in which exchange interactions within a single particle exceed magnetic interactions between the particles. The experimental preparation technique of such systems allows both the particle's size and average distance between them to be controlled within a wide range.[21] Because of the presence of magnetic anisotropy energy or shape energy for particles of cubic symmetry, the magnetic moment of a single particle influenced by an external variable magnetic field cannot change its direction continuously and fluctuates between directions along the easiest magnetization axis. In general, such fluctuations are random in character and do not occur simultaneously for all particles. Moreover, in reality there are usually distributions of particles over directions of the easiest magnetization axis (texture), volumes, and local nearest neighborhoods in the systems. The hyperfine fields $H_{\rm hf}$ at nuclei in such a system obviously follow changes in magnetic moments of particular particles and not those in the magnetic moment of the whole sample. Since the direction of a magnetic moment for a single particle changes in time stochastically, the $H_{\rm hf}(t)$ direction also will change to some extent in time randomly. The relaxation model for a single magnetic particle and a particle system will be determined in the next section, and right now we come to a derivation of the general expression for absorption Mössbauer spectra based only on the stochastic character of $H_{\rm hf}(t)$.

Let the time-dependent hyperfine field $H_{\rm hf}(t)$ influence a nucleus. Suppose it is always parallel to a certain z axis while its value can vary arbitrarily including changes in sign to opposite one. In this case the Hamiltonian of the system can be written as

$$\hat{H} = \hat{H}_0 + g\mu_N \hat{I}_z H_{\rm hf}(t) + \hat{V}_{\gamma N}(t_0), \tag{1}$$

where the Hamiltonian $\hat{H}_0$ describes the energy levels of a nucleus in ground and excited states with no hyperfine interaction; the second term describes the hyperfine interaction. Here g is the nuclear g factor, μ_N is the nuclear magneton, I_z is the projection of nuclear spin on the hyperfine field direction; $\hat{V}_{\gamma N}(t_0)$ describes the interaction between the γ quantum and nucleus, and t_0 is the switching on time of the interaction.[22] The time t_0 is usually ignored, but there is the time-dependent rf field in our case, which has its zero time reference; so t_0 should be retained.

The wave functions of the ground $\psi_m(t)$ and excited $\psi_M(t)$ nuclear states in the time-dependent hyperfine field can be defined as

$$\psi_m(t)=\exp\left[-ig_g\mu_N m\int_{t_0}^{t}H_{\rm hf}(t')dt'\right]|m\rangle, \tag{2}$$

$$\psi_M(t)=\exp\left[-ig_e\mu_N M\int_{t_0}^{t}H_{\rm hf}(t')dt' + \left(i\frac{E_0}{\hbar}-\frac{\Gamma_0}{2}\right)(t-t_0)\right]|M\rangle.$$

Here $g_g\mu_N$ and $g_e\mu_N$ are the nuclear magnetic moments, m and M are the projections of nuclear spin on the hyperfine field direction in the ground and excited states, corresponding, and E_0 and Γ_0 are the energy and width of the excited nuclear level.

According to the general theory of the resonant radiation,[22] the amplitude of absorption of the γ quantum with energy $E=\hbar\omega$ is given by

$$c_{mM}(\omega)=\int_{t_0}^{\infty}\langle\psi_M^*(t)|\hat{V}_{\gamma N}(t_0)e^{i\omega(t-t_0)}|\psi_m(t)\rangle dt \equiv V_{mM}\int_{t_0}^{\infty}\exp\left[\int_{t_0}^{t}i\omega_{mM}(t')dt'+i\tilde{\omega}(t-t_0)\right]dt, \tag{3}$$

where $\omega_{mM}(t)=(g_eM-g_gm)\mu_N H_{\rm hf}(t)$, $\tilde{\omega}=\omega+i\Gamma_0/2$, and V_{mM} are the matrix elements of the nuclear current operator, which include the Mössbauer effect probability. The squared modulus of the absorption amplitude is used to define the absorption cross section.[22] However, such a procedure is adequate only with no external perturbations like a rf field. In the presence of a rf field, the averaging over zero time t_0 must be done. Because of the strict periodicity of the rf field, it is obvious that the averaging should be performed within one period. Then the absorption cross section can be written as

$$\sigma(\omega)=\sigma_a\sum_{\alpha}|\tilde{N}_\alpha|^2\varphi(\alpha,\omega), \tag{4}$$

where

$$\varphi(\alpha,\omega)=\frac{1}{T_{\rm rf}}\int_0^{T_{\rm rf}}\left\langle\left|\int_{t_0}^{\infty}\exp\left\{\int_{t_0}^{t}i[\tilde{\omega}-\omega_\alpha(t')]dt'\right\}dt\right|^2\right\rangle dt_0 \equiv\frac{1}{T_{\rm rf}}\int_0^{T_{\rm rf}}dt_0\int_{t_0}^{\infty}dt_1\,\exp[-\Gamma_0(t_1-t_0)]\int_{t_1}^{\infty}dt \times\left\langle\exp\left\{\int_{t_1}^{t}i[\tilde{\omega}-\omega_\alpha(t')]dt'\right\}\right\rangle+\text{c.c.} \tag{5}$$

Here $\sigma_a=f_a n_a\sigma_0 t_a$ is the effective absorber thickness, f_a is the probability of the Mössbauer effect in the absorber, n_a is the density of resonant nuclei in the absorber, σ_0 is the transverse resonant absorption cross section, and t_a is the absorber thickness; $\alpha=(m,M)$; the coefficients C_α denote the intensities of the corresponding transitions and are defined through the Clebsch-Gordan coefficients; $T_{\rm rf}=2\pi/\omega_{\rm rf}$ is the rf-field period.

Along with averaging over the rf-field period in Eq. (5), stochastic averaging over different time trajectories of $H_{\rm hf}(t)$ is to be performed, which is denoted as the brackets in Eq. (5). In order to understand clearly the way of solving of the problem, we will consider the case with no rf field and render the deduction following the procedure suggested by Anderson.[23,24] According to the latter, we assume that the function $H_{\rm hf}(t)$ is given by a uniform Markoff process; that is, the hyperfine field $H_{\rm hf}(t)$ can take on n discrete values $H_{\rm hf}^{(k)}$ and fluctuates stochastically between them. Moreover, it is assumed that the probability of a transition from the state k_1 to k_2 for a small time interval Δt is given as

$$P_{k_1k_2}(\Delta t)=p_{k_1k_2}\Delta t \quad \text{at } k_1\neq k_2, \tag{6}$$

where $p_{k_1k_2}$ is the probability of the k_1 to k_2 transition per unit time. Then the probability to stay within the current state for Δt is defined by the obvious condition

$$\sum_{k_2}P_{k_1k_2}(\Delta t)=1, \tag{7}$$

whence it appears

$$P_{k_1k_1}(\Delta t)=1-\sum_{k_1\neq k_2}p_{k_1k_2}\Delta t. \tag{8}$$

In this case the stochastic averaging over different time trajectories of $H_{\rm hf}(t)$ in Eq. (5) is reduced to averaging over all possible combinations of transitions between the states $H_{\rm hf}^{(k)}$. Let us divide the time interval (t_1,t) into n equally spaced Δt steps. In accordance with what is mentioned above, the expression in the brackets in Eq. (5) can be written as

$$\left\langle\exp\left\{\int_{t_1}^{t}i[\omega-\omega_\alpha(t')]dt'\right\}\right\rangle =\sum_{k,k_1,\ldots,k_n}W_k(t_1)e^{i(\tilde{\omega}-\omega_\alpha^{(k)})\Delta t}P_{kk_1}(\Delta t) \times e^{i(\tilde{\omega}-\omega_\alpha^{(k_1)})\Delta t}\ldots P_{k_{n-1}k_n}(\Delta t). \tag{9}$$

Here $\omega_\alpha^{(k)}=(g_eM-g_gm)\mu_N H_{\rm hf}^{(k)}$, and $W_k(t_1)$ is the population of the state k at t_1. For the subsequent work it is convenient to introduce the matrix of hyperfine transitions $\hat{\omega}_\alpha$ and the relaxation matrix $\hat{P}$, which are determined as

$$(\hat{\omega}_\alpha)_{kk_1}=\omega_\alpha^{(k)}\delta_{kk_1}, \tag{10}$$

$$(\hat{P})_{kk_1}=p_{kk_1} \quad \text{at } k\neq k_1, \tag{11}$$

$$(\hat{P})_{kk}=-\sum_{k_1\neq k} p_{kk_1}. \tag{12}$$

Taking into account the notation and Eq. (8), Eq. (9) can be reduced to the matrix representation

$$\left\langle \exp\left\{ \int_{t_1}^{t} i[\tilde{\omega}-\omega_\alpha(t')]dt' \right\} \right\rangle = \langle W(t_1)| \prod_k e^{i[\tilde{\omega}-\hat{\omega}_\alpha-\hat{P}(t_k)]\Delta t}|1\rangle, \tag{13}$$

where $t_k=t_1+(k-1)\Delta t$, $\langle W(t_1)|$ is the population vector, and $|1\rangle$ is the unity column.

In the absence of a rf field, the relaxation constants as well as the operator $\hat{P}$ do not depend on time. Besides that, $\langle W(t)|$ are the equilibrium population vectors and are also time independent. Then Eq. (13) can be reduced to the expression

$$\left\langle \exp\left\{ \int_{t_1}^{t} i[\tilde{\omega}-\omega_\alpha(t')]dt' \right\} \right\rangle = \langle W_0|e^{i(\tilde{\omega}-\hat{\omega}_\alpha-\hat{P})(t-t_1)}|1\rangle, \tag{14}$$

and, correspondingly, Eq. (5) becomes of the simple form

$$\varphi(\alpha,\omega)=\frac{1}{\Gamma_0}\left\langle W_0\left|\frac{i}{\tilde{\omega}-\hat{\omega}_\alpha+i\hat{P}}\right|1\right\rangle+\text{c.c.} \tag{15}$$

This is the conventional representation of the relaxation Mössbauer spectra, based on which the absorption spectra are practically analyzed in most of the works (see, for instance, the review in Ref. 25).

III. RELAXATION MÖSSBAUER SPECTRA UNDER rf MAGNETIC-FIELD EXCITATION: GENERAL EQUATIONS

Let us have a look at Eq. (5). Taking into account the periodicity of the rf field, it can be transformed to an essentially simpler form. The integration over t_0 can be performed by parts, which results in

$$\begin{aligned}\varphi(\alpha,\omega)=\frac{1}{\Gamma_0 T_{\rm rf}}\Bigg\{ &\int_0^{T_{\rm rf}} dt_1 \int_{t_1}^{\infty} dt \\ &\times\left\langle \exp\left\{ \int_{t_1}^{t} i[\tilde{\omega}-\omega_\alpha(t')]dt' \right\} \right\rangle \\ &+\int_0^{\infty} dt_1 e^{-\Gamma_0 t_1}\int_{t_1}^{\infty} dt \\ &\times\left[\left\langle \exp\left\{ \int_{t_1}^{t} i[\tilde{\omega}-\omega_\alpha(t'+T_{\rm rf})]dt \right\} \right\rangle \right. \\ &\left. -\left\langle \exp\left\{ \int_{t_1}^{t} i[\tilde{\omega}-\omega_\alpha(t')]dt' \right\} \right\rangle \right] \Bigg\}+\text{c.c.}\end{aligned} \tag{16}$$

From the periodicity of rf field, it can be easily shown that the second term in Eq. (16) is canceled and this equation is reduced to the form

$$\begin{aligned}\varphi(\alpha,\omega)=\frac{1}{\Gamma_0 T_{\rm rf}}&\int_0^{T_{\rm rf}} dt_1 \int_{t_1}^{\infty} dt \\ &\times\left\langle \exp\left\{ \int_{t_1}^{t} i[\tilde{\omega}-\omega_\alpha(t')]dt' \right\} \right\rangle+\text{c.c.}\end{aligned} \tag{17}$$

The expression of the stochastic average in the brackets with regards to the time-dependent relaxation parameters has been obtained in the previous section and is determined by Eq. (13). The averaging procedure hardly differs from that for the relaxation parameters being constant. However, in this case we cannot come from Eq. (13) to Eq. (14).

Let us introduce the operator

$$\begin{aligned}\hat{G}(t_1,t)&=\lim_{\Delta t\to 0}\prod_{k=1}^{n} e^{i[-\hat{\omega}_\alpha-\hat{P}(t_k)]\Delta t} \\ &=\hat{T}\exp\left\{ \int_{t_1}^{t} dt'[-i\hat{\omega}_\alpha-\hat{P}(t')] \right\},\end{aligned} \tag{18}$$

where $\hat{T}$ is the time-ordering operator which acts following the rule

$$\hat{T}A(t)B(t')=\begin{cases} A(t)B(t'), & t>t', \\ B(t')A(t), & t'>t. \end{cases}$$

In accordance with the definition and the periodicity of the rf field, the operator $\hat{G}(t_1,t)$ has the properties

$$\hat{G}(t_1,t)=\hat{G}(t_1,t_2)\hat{G}(t_2,t) \quad \text{at } t_1<t_2<t, \tag{19}$$

$$\hat{G}(t_1+T_{\rm rf},t+T_{\rm rf})=\hat{G}(t_1,t). \tag{20}$$

Taking into account Eqs. (9) and (18), Eq. (5) is reduced to

$$\varphi(\alpha,\omega)=\frac{1}{\Gamma_0 T_{\rm rf}}\int_0^{T_{\rm rf}} dt_1 \int_{t_1}^{\infty} dt \langle W(t_1)|e^{i\tilde{\omega}(t-t_1)}\hat{G}(t_1,t)|1\rangle + \text{c.c.} \tag{21}$$

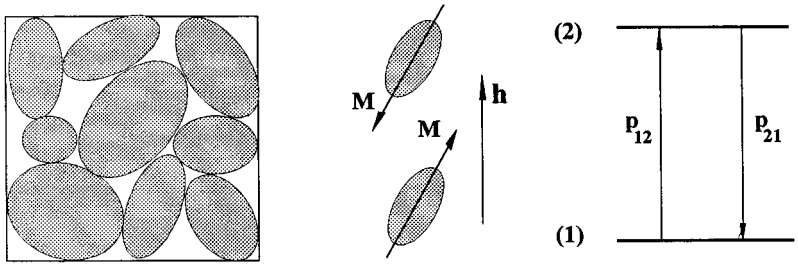

FIG. 1. State of a particle with opposite directions of the magnetic moment **M** in external magnetic field **h** [(a,b)] and scheme of the transitions between these two states (b).

Taking into consideration Eqs. (19) and (20), Eq. (21) can be reduced to a form that is more convenient for practical calculations:

$$\varphi(\alpha,\omega)=\frac{1}{\Gamma_0 T_{\rm rf}}\int_0^{T_{\rm rf}}dt_1\int_{t_1}^{t_1+T_{\rm rf}}dt \times\langle W(t_1)|\frac{\exp[i\tilde{\omega}(t-t_1)]}{1-\exp(i\tilde{\omega}T_{\rm rf})\hat{G}(t_1,t_1+T_{\rm rf})} \times\hat{G}(t_1,t)|1\rangle+\text{c.c.} \quad (22)$$

This representation where integration is performed in finite terms is the most appropriate for computer calculations. Actually, Eqs. (21) and (22) replace the known Singwi-Sjolander equation[26] when the sample is subjected to a variable magnetic field. This result *solves the considered problem completely* and delivers the shape of absorption Mössbauer spectra in the presence of relaxation and rf-field perturbation, provided that the magnetic dynamics of the system is known. In general form, the time evolution of the population vector $\langle W(t_1)|$ is described by the equation

$$\langle W(t_1)|\hat{G}_0(t_1,t)=\langle W(t)|, \quad (23)$$

where $\hat{G}_0(t_1,t)$ is determined by Eq. (18) at $\omega_\alpha=0$. Equations (21)–(23) can be used for a wide variety of relaxation processes.

IV. RELAXATION MODEL AND DYNAMICS OF A MAGNETIC SYSTEM

In the following we propose an example of a model describing the magnetic relaxation processes in a ferromagnet. Let us consider a ferromagnet as an ensemble of Stoner-Wohlfarth particles and suppose that exchange interactions within a single particle exceed the exchange and/or dipole-dipole interactions between the particles. The interaction between particles will be taken into consideration within the molecular-field approximation, in which the interaction is described in terms of an exchange field $h_{\rm ex}$ proportional to the magnetization $M(t)$ of the whole sample:

$$h_{\rm ex}=c_{\rm ex}M(t), \quad (24)$$

where $c_{\rm ex}$ is a factor that determines the Curie temperature as seen below. If the particles are of the same kind, equal volume, and the sample's bulk is closely packed with the particles, $M(t)$ coincides with the specific magnetization of a single particle.

Along with the exchange interaction, the magnetic anisotropy energy of a particular particle should be taken into consideration, which is used to be determined as

$$E_{\rm an}=KV_0\sin^2\theta, \quad (25)$$

where K is the magnetic anisotropy energy constant, V_0 is the volume of the particle, and θ is the angle between the magnetization vector and its easy direction in the particle. Below, we will suppose that the magnetic anisotropy energy is much greater than temperature:

$$KV_0\gg k_BT. \quad (26)$$

If the condition is valid, then such a particle may stay only in two states with opposite directions of its magnetic moment. Under thermal fluctuations the particle jumps from one state to another (see Fig. 1). With neither external magnetic field nor the exchange interaction between the particles, these states are equally populated, and the transition frequencies p_{12} and p_{21} are equal to each other. In an external magnetic field h, the states appear to be variously populated:

$$w^0_{1,2}=\frac{\exp(\pm E_h/k_BT)}{\exp(E_h/k_BT)+\exp(-E_h/k_BT)}, \quad (27)$$

where

$$E_h=M_0V_0h \quad (28)$$

and M_0 is the specific saturation magnetization of a single particle.

In accordance with Eqs. (27) and (28), the equilibrium magnetic moment of a particle is determined by the equation

$$m_0(T)=M_0(T)/M_0\tanh(M_0V_0h/k_BT). \quad (29)$$

In the absence of an external field, $h=h_{\rm ex}$, and according to Eq. (24), we find

$$m_0(T)=\tanh[m_0(T)T_C/T], \quad (30)$$

where

$$T_C=M_0^2V_0c_{\rm ex}/k_B. \quad (31)$$

Here T_C is the Curie temperature. In the paramagnetic range at $T>T_C$ only the trivial solution $M_0(T)=0$ exists, while at $T<T_C$, in the ferromagnetic state, a nonzero solution exists. In our case, in a system of identical particles, $M_0(T)$ is just the specific magnetization of the whole sample.

In an external magnetic field h, along with changes in the equilibrium populations, the probabilities of transitions be-

tween the equilibrium states change too and become functions of the applied field. Determination of the field dependences of the relaxation parameters is a quite complicated problem.[27] However, the relation between the relaxation parameters, which is defined by the detailed balancing principle, remains valid:

$$w_1^0 p_{12} = w_2^0 p_{21}. \tag{32}$$

For definition, we suppose that the energy of magnetic interactions is rather smaller than the magnetic anisotropy energy, that is,

$$E_h \ll E_{\rm an}. \tag{33}$$

In this case the probabilities of transitions can be written as

$$p_{12} = p_0 \exp[(-E_{\rm an} + E_h)/k_B T],$$
$$p_{21} = p_0 \exp[(-E_{\rm an} - E_h)/k_B T], \tag{34}$$

where p_0 is a constant. Equations (34) will be used for the calculation of both the magnetization curves and Mössbauer spectra. Since the relaxation process in this case is of under barrier nature, the external magnetic field may change the relaxation parameters by several orders of magnitude. Note that for strong magnetic fields more accurate equations can be used.[27]

As easily seen from Eqs. (23), the time evolution of the magnetic moment of a particle subjected to an external rf field,

$$h_{\rm rf}(t) = h_0 \cos(\omega_{\rm rf} t), \tag{35}$$

is described within a simple equation

$$\frac{dm(t)}{dt} = -p(t)[m(t) - m_0(T)], \tag{36}$$

where

$$m(t) = M(t)/M_0, \quad p(t) = p_{12}(h(t)) + p_{21}(h(t)),$$

and $m_0(t)$ is given by Eq. (29), in which h is to be replaced by

$$h = h_{\rm ex} + h_{\rm rf}(t). \tag{37}$$

Equation (36) is to be supplemented with initial conditions. In our case the latter is the periodic boundary condition

$$m(t + T_{\rm rf}) = m(t). \tag{38}$$

In solving the nonlinear equation (36), one should use Eq. (29), along with Eq. (38). Examples of the solution of these equations will be presented in the following sections including the hysteresis curves.

Let us turn to the general equations (21) and (22). The matrix $i\hat{\omega}_\alpha + \hat{P}(t)$ that appears therein can be written as

$$i\hat{\omega}_\alpha + \hat{P}(t) = \begin{pmatrix} i\omega_\alpha + p_{12}(t) & -p_{12}(t) \\ -p_{21}(t) & -i\omega_\alpha + p_{21}(t) \end{pmatrix}, \tag{39}$$

and the population vector components are determined as

$$w_{1,2}(t) = \tfrac{1}{2}[1 \pm m(t)]. \tag{40}$$

Taking into account that $m(t)$ can be evaluated according to the procedure discussed above, Eqs. (39) and (40) allow the absorption Mössbauer spectra to be calculated.

V. FAST RELAXATION REGIME

As can be understood from the above, the shape of absorption Mössbauer spectra is a complicated function of the rf-field frequency and strength, Larmor frequencies, and relaxation parameters as well. In the general case calculations of the spectra are rather extensive, and the general equations cannot be simplified without any assumptions. However, in several limiting cases, two of which will be considered below, Eqs. (21) and (22) can be greatly simplified.

Let us consider a situation when the relaxation process is extremely fast so that the parameter

$$p^{(0)} = p_0 \exp(-E_{\rm an}/k_B T), \tag{41}$$

which determines an ''initial'' relaxation of ferromagnetic particles with no external magnetic field, appears to be much greater than both the rf-field frequency and Larmor frequency:

$$p^{(0)} \gg \omega_{\rm rf}, \omega_\alpha. \tag{42}$$

In the limit of high $p^{(0)}$ one can neglect the left part of Eq. (36) and get

$$m(t) = M(t)/M_0 = \tanh[(m(t) + h_{\rm rf}(t)/h_{\rm ex}^{(0)}) T_C/T], \tag{43}$$

where $h_{\rm ex}^{(0)} = c_{\rm ex} M_0$.

Suppose that the sample's temperature is below T_C. Then there are two qualitatively different kinds of solution of Eq. (36) as a function of the rf-field strength h_0. At h_0 greater than a threshold field h_a, Eq. (36) has the only solution symmetrical with respect to time reversal. At $h_0 < h_a$ there exist two solutions, each of which transforms into the other with time reversal. It can be easily found that the threshold field is determined from

$$h_a = h_{\rm ex}^{(0)} \left\{ \sqrt{1 - T/T_C} - \frac{T}{2T_C} \ln\left[\frac{2T_C}{T} (1 + \sqrt{1 - T/T_C}) - 1 \right] \right\}. \tag{44}$$

Naturally, h_a depends on temperature and the dependence is shown in Fig. 2. The characteristic magnetization curves as hysteresis loops are shown in Fig. 3. In high fields h_0 the hysteresis behavior corresponds to simple physical conceptions. The field h_0 breaks off the exchange interactions, and due to the fast relaxation processes, the particle's magnetic moment has time to change its direction, which results in the hysteresis curve being symmetrical with respect to time reversal. In a small magnetic field insufficient for magnetization reversal, the magnetic moment of a particle as well as

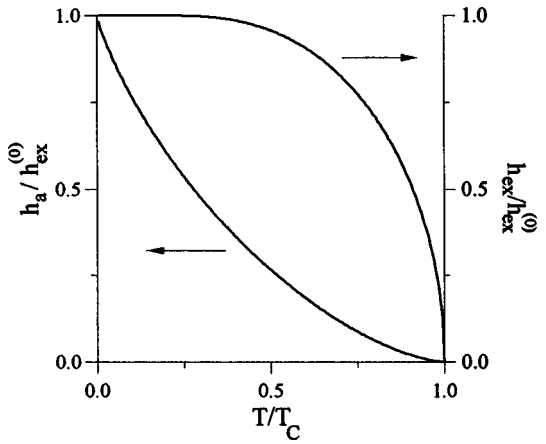

FIG. 2. Temperature dependence of the threshold field h_a and exchange field $h_{\rm ex}$ normalized to $h_{\rm ex}^{(0)}$.

that of the whole sample may slightly oscillate around its equilibrium state which is, generally speaking, determined by the initial state of the whole sample or particular domain. In a ferromagnet, there are two such states with opposite directions of the sample's magnetic moment with respect to the rf magnetic-field axis. In principle, the states are absolutely equivalent, but either the initial state of the whole sample before rf-field switching on or an additional small magnetic field predetermines the alternative of the two solutions. The transition from one regime to another occurs at definite values of h_0 when the sample's state with the magnetic moment direction opposite to the rf-field direction becomes absolutely unstable. Within the fast relaxation limit, the system falls down to the state with the magnetic moment aligned parallel with the rf field applied at the moment. In this case, a distinctive symmetry breaking of the magnetic system in the external rf field takes place. It is similar to thermodynamical considerations concerning the broken symmetry in ferromagnets. Here it is, on principle, impossible to determine the direction of a magnetic moment of the whole sample (or a particular domain) while an extremely small constant magnetic field predetermines the direction. When the relaxation processes are not extremely fast, the transition from one regime to another is going on more or less smoothly (see Fig. 4). Note that the value of the threshold field in the whole temperature range, except for the low-temperature region, appears to be considerably smaller than the temperature averaged and exchange field $h_{\rm ex}(T) = h_{\rm ex}^{(0)} M(T)/M_0$, the temperature dependence of which is also presented in Fig. 3.

Now let us turn to Eq. (18). Let $\lambda_i(t)$ be the eigenvalues, and $|u^{(i)}(t)\rangle$ and $\langle v^{(i)}(t)|$ be the right and left eigenvectors of the matrix $i\hat{\omega}_\alpha + \hat{P}(t)$. Then each factor in Eq. (18) can be represented in the form

$$e^{i[-\hat{\omega}_\alpha - \hat{P}(t_k)]\Delta t} = \sum_{j=1}^{n} e^{-i\lambda(t_k)} |u^{(1)}(t_k)\rangle\langle v^{(f)}(t_k)|. \quad (45)$$

In the case of a two-level system, the matrix $i\hat{\omega}_\alpha + \hat{P}(t)$ is represented by Eq. (45) where in the fast relaxation limit

$$p = p_{12} + p_{21} \gg \omega_\alpha \quad (46)$$

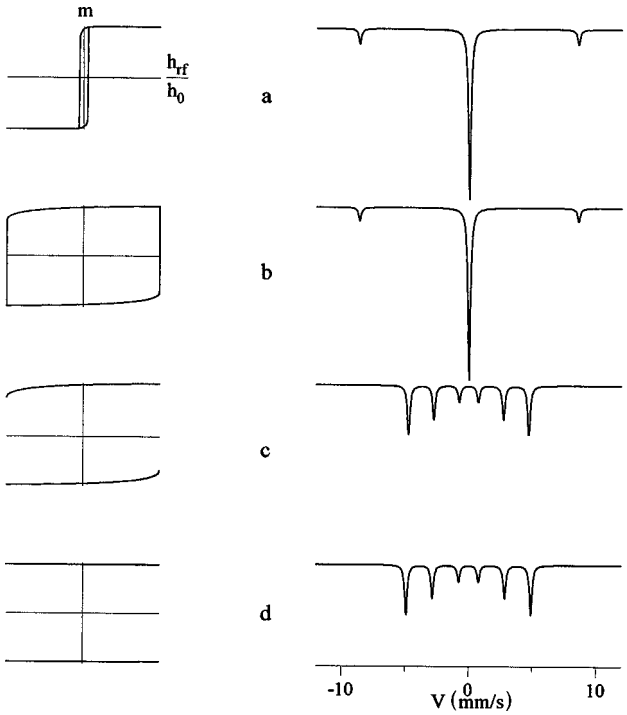

FIG. 3. Magnetization curves (left) in a 100-MHz rf field at $T/T_C = 0.5$ for different rf-field strengths: $h_0/h_{\rm ex} = 5.0$, 0.2665, 0.2664, and 0.01 from (a) to (d) and corresponding absorption Mössbauer spectra (right) at $\omega_L = 60$ MHz in the fast relaxation regime.

and the eigenvalues and eigenvectors are easily found to be

$$\lambda_1(t) = \overline{\omega_\alpha}(t) = \omega_\alpha m(t), \quad |u^{(1)}(t)\rangle = \begin{pmatrix} 1 \\ 1 \end{pmatrix},$$

$$\langle v^{(1)}(t)| = (w_1(t), w_2(t)),$$

$$\lambda_2(t) = p, \quad |u^{(2)}(t)\rangle = \begin{pmatrix} -w_2(t) \\ w_1(t) \end{pmatrix}, \quad \langle v^{(2)}(t)| = (-1,1), \quad (47)$$

where $w_{1,2}(t)$ is defined by Eq. (40). If the inequality (46) is held, the only term with $j=1$ in the sum over j on the right of Eq. (45) can be kept, the other terms vanishing in the fast relaxation limit. As a result, the operator $\hat{G}(t_1,t)$ is defined by the simple equation

$$\hat{G}(t_1,t) = \exp\left[-i \int_{t_1}^{t} \overline{\omega_\alpha}(t')dt' \right] \begin{pmatrix} w_1(t) & w_2(t) \\ w_1(t) & w_2(t) \end{pmatrix}. \quad (48)$$

Then, a new representation of the function $\varphi(\alpha,\omega)$ from Eq. (21) is easily found to be

$$\varphi(\alpha,\omega) = \frac{1}{\Gamma_0 T_{\rm rf}} \int_0^{T_{\rm rf}} dt_1 \int_0^{\infty} dt \times \exp\left\{ -i \int_0^t [\tilde{\omega} - \overline{\omega_\alpha}(t'+t_1)]dt' \right\} + \text{c.c.} \quad (49)$$

This equation by analogy with Eq. (22) is reduced to a form more appropriate for concrete calculations:

$$\varphi(\alpha,\omega)=\frac{1}{\Gamma_0 T_{\rm rf}}\int_0^{T_{\rm rf}}dt_1\int_0^{T_{\rm rf}}dt \times\frac{\exp[i\tilde{\omega}t-i\int_0^t\overline{\omega_\alpha}(t'+t_1)dt']}{1-\exp[i\tilde{\omega}T_{\rm rf}-i\int_0^{T_{\rm rf}}\overline{\omega_\alpha}(t'+t_1)dt']}+\text{c.c.} \tag{50}$$

Note that Eqs. (49) and (50) do not include the populations $w_{1,2}(t)$ which appear in the initial equations (21) and (22): however, the magnetism does not vanish completely, but is involved in the equations for the absorption spectra through the function $\overline{\omega_\alpha}$ defined within Eq. (47).

Figure 3 shows also the absorption Mössbauer spectra for different values of the rf-field strength h_0, which have been calculated within Eqs. (4) and (50). At high h_0 much greater than $h_{\rm ex}$, when the external rf field breaks off the exchange interactions, the magnetization reversal, suggested by Pfeiffer as a condition to observe the collapse effect, is realized. That is, the sample's magnetic moment follows the external rf field almost everywhere, except for a small $h_{\rm rf}(t)$ range [Fig. 3(a)]. When the rf-field direction changes to the opposite one, the magnetic moment changes its direction almost simultaneously to the opposite. Besides that, according to Eq. (47), the hyperfine field at the nuclei always follows the sample's magnetic moment. For the whole rf-field period, the hyperfine field is completely averaged to zero so that the resulting absorption spectrum looks like a single line accompanied by weak sidebands, which is in accordance with earlier theoretical predictions. With decreasing h_0 the hysteresis curves change in shape, and in the vicinity of the threshold field h_a the magnetic moment does not completely follow the rf field [Fig. 3(b)], but for half the time $m(t)$ appears to be oriented in the direction opposite with respect to the rf-field direction. Nevertheless, as seen from Fig. 3(b), the collapse effect is realized in a complete manner with slight changes in the line shape. *Thus, in order to observe the complete collapse effect, it is sufficient that the hyperfine field be averaged to zero for the rf-field period and it is not necessary that the magnetic moment totally follow the rf field*. Besides that, a rather weak rf-field strength considerably smaller than the exchange field one is quite enough to give rise to the collapse effect. With further decreasing h_0, just at the point where it becomes smaller than h_a, the process of magnetization reversal changes abruptly in character, as has been discussed already, and a well-resolved sextet appears in the absorption spectra [Fig. 3(c)]. At lower h_0 values the magnetization curve and the spectra change slightly. Thus, in the fast relaxation limit, the collapse effect is of pronounced threshold character. At $h_0<h_a$ the well-resolved hyperfine structure is to be observed, while at $h_0>h_a$ the collapsed spectrum is revealed.

When the relaxation is not extremely fast, the general equation (22) should be used to calculate the absorption spectra. In this case the external-field dependence of the relaxation constants must be known, and Eqs. (36) and (39) will be used below. Figure 4 shows the magnetization curves and absorption Mössbauer spectra for the case when the relaxation constant $p^{(0)}$ is only twice greater than the rf-field frequency. In this situation it is already possible to trace the characteristic features of the transition from the collapsed line to the resolved spectrum. In approaching the threshold point from high-rf-field strength, a strong broadening of the spectrum occurs, and as seen from Figs. 4(b) and 4(c), the intensities of sidebands decrease. A similar picture reveals in approaching h_a from weak fields h_0, a partial averaging of the hyperfine field and broadening of particular spectral lines occur [Figs. 4(c) and 4(d)], the outmost lines being broadened more strongly than the inner ones. Note that even in this case, when the relaxation process is not so fast and $p^{(0)}$ is only twice the rf-field frequency, the transition takes place in a rather narrow range of the rf-field strength. The rf-field strengths for Figs. 4(b) and 4(d) differ only by several fractions of a percent. Nevertheless, the transition interval is already much broader than that in the fast relaxation limit where the transition width $\Delta h/h_a$ can be very small in the range of about 10^{-7}.

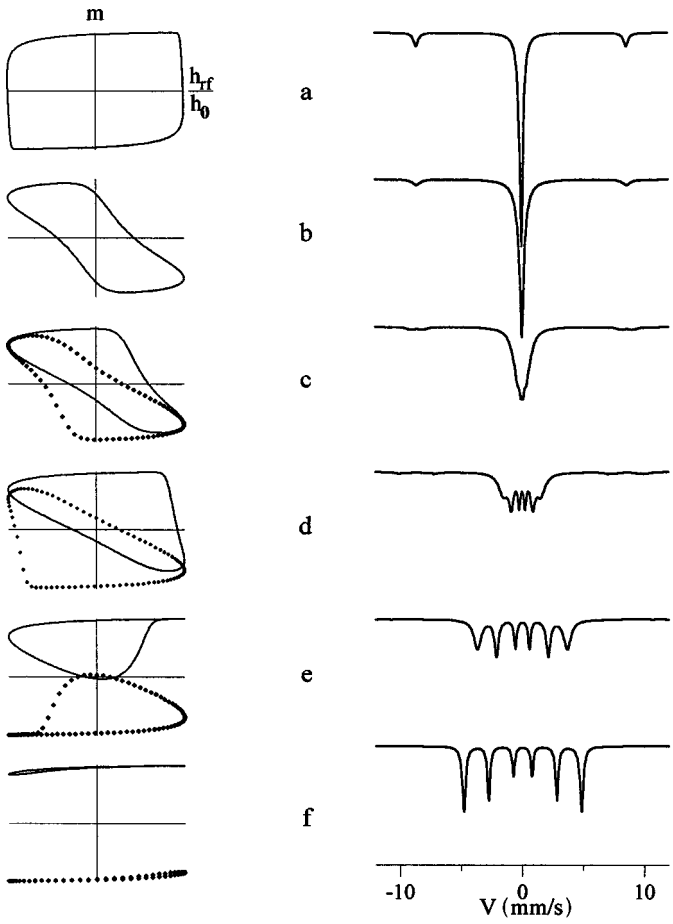

FIG. 4. Magnetization curves (left) in the 100-MHz rf field at $T/T_C=0.5$ for different rf-field strengths: $h_0/h_{\rm ex}=0.4$, 0.327, 0.3263, 0.3262, 0.326, and 0.25 from from (a) to (f) and corresponding absorption Mössbauer spectra (right) at $\omega_L=60$ MHz in the fast, but finite relaxation regime at $p^{(0)}=200$ Mhz.

VI. MULTIPHASE SYSTEMS

It is obvious that in real situations it is difficult to find a system that consists of identical particles. Indeed, there are

spreads in the volume V_{0i} and the orientation of particles $\mathbf{n}_i$ as well as the system may contain a number of different phases which differ in the specific saturation magnetic moments M_{0i}, the anisotropy energy, and, therefore, the relaxation parameters $p_i(t)$, and also in the constants $c_{\rm ex}^{(i)}$. The dynamics of a magnetic system will be described by combined equations like Eq. (36) for particles of different kinds:

$$\frac{dM_i(t)}{dt} = -p_i(t)[M_i(t) - M_{0i}(T)], \tag{51}$$

where the index i denotes particles of a particular kind and $\mathbf{n}_i$ is the unit vector along the ith magnetic moment direction. Then the sample's magnetic moment can be determined as

$$M(t) = \sum_i g_i M_i \mathbf{n}\mathbf{n}_i, \tag{52}$$

where $\mathbf{n}$ is the unit vector along the sample's magnetic moment direction, which is supposed to be aligned along the magnetic rf field, and g_i is the weight factor for particles of the ith kind. With that the ''equilibrium'' magnetic moment of a particle will be defined through the average one by means of

$$M_{0i}(T) = M_{0i}\tanh\left[\alpha_{ci}\tilde{h}_i(t)\,\frac{T_C}{T}\right] \tag{53}$$

where

$$\tilde{h}_i(t) = [m(t) + h_{\rm rf}(t)/h_{\rm ex}^{(0)})\mathbf{n}\mathbf{n}_i,$$

$$m(t) = \sum_i g_i M_i(t)\mathbf{n}\mathbf{n}_i \Big/ \sum_i g_i M_{0i}\mathbf{n}\mathbf{n}_i,$$

$$k_B T_C = \sum_i g_i c_{\rm ex}^{(i)} V_{0i} M_{0i}^2 (\mathbf{n}\mathbf{n}_i)^2,$$

$$h_{\rm ex}^{(0)} = \sum_i g_i c_{\rm ex}^{(i)} M_{0i}\mathbf{n}\mathbf{n}_i,$$

$$\alpha_{ci} = M_{0i}V_{0i}\sum_k g_k M_{0k}\mathbf{n}\mathbf{n}_k \Big/ \sum_k g_k M_{0k}^2 V_{0k}(\mathbf{n}\mathbf{n}_k)^2.$$

Note that Eqs. (51) are not independent, but coupled in a nonlinear manner through Eqs. (52). Nevertheless, the solution of such equations, when the number of them is not exceeding 100, can be performed even using personal computers.

As an example, consider the case when the sample is a single-phase magnetic system consisting of particles of equal volume, but their easiest magnetization axes are distributed uniformly over all directions. The corresponding magnetization curves and absorption spectra for two close values of the rf-field strength are shown in Figs. 5(a) and 5(c). Additionally, the hysteresis curves and corresponding partial spectra for particles whose easiest magnetization axes are oriented

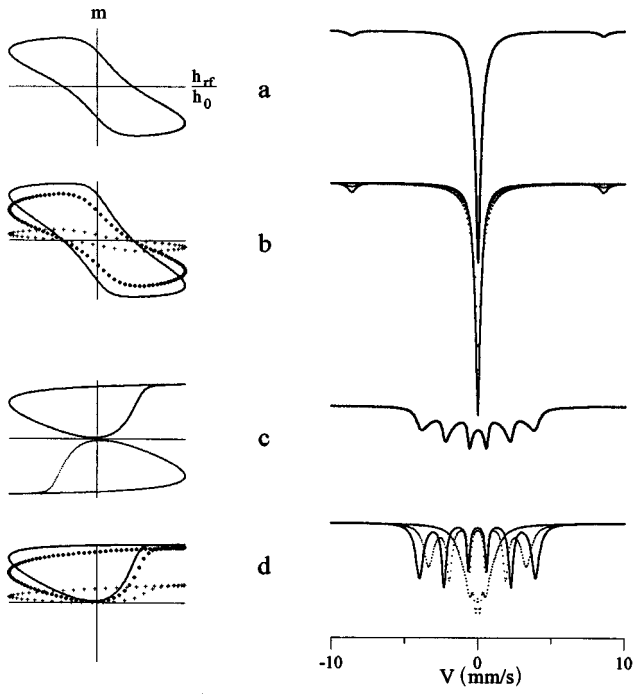

FIG. 5. Magnetization curves and Mössbauer spectra in the 100-MHz rf field with $h_0/h_{\rm ex}=0.2910$ (a) and 0.2905 (c) at $T/T_C=0.5$, $\omega_L=60$ MHz, and $p^{(0)}=200$ MHz for a distribution of easiest magnetization axes of particular particles. (b), and (d) are the corresponding partial magnetization curves and subspectra for particles with $\theta=10°$ (crossed line), 45° (dotted line), and 80° (solid line). Dual solution is not presented in (d).

by the angle $\theta=10°$, 45°, and 80° with respect to the rf-field direction are shown [Figs. 5(b) and 5(d)]. As seen from the figure, for each group of particles the hysteresis curves differ, but they are similar to each other and to that for the whole sample in their character. That is, at h_0 greater than a threshold field all the curves are symmetrical in time reversal, and at h_0 lower than the threshold field there are two solutions, which transform one into another with time reversal, for both particles of a certain kind and the whole sample. [There are no dual solutions in Fig. 5(d) from visual aids.] Figure 6 shows the absorption Mössbauer spectra in a wider range of the rf-field strengths. Despite the character of the hysteresis curves changing abruptly with h_0 crossing the threshold field, there are no sharp changes in the spectra within the field transition, as has been observed above for the case of a single particle, and a rather smooth transition from the collapsed line to the resolved hyperfine structure occurs. The character of this transition differs qualitatively for the approach to the transition point from high and low fields h_0. In a strong rf field, a narrow single line is observed together with weak sidebands. Their appearance in the high h_0 limit is according with the results of earlier theoretical calculations,[16] while with h_0 decreasing the central line broadens to some extent and the intensities of sidebands decreases. In approaching the threshold field, the intensities of the sidebands practically vanish. It is clear from the above analysis that it is hardly possible to derive any simple description of the field dependence of the intensities of sidebands. In the region of low rf field, the transition appears to

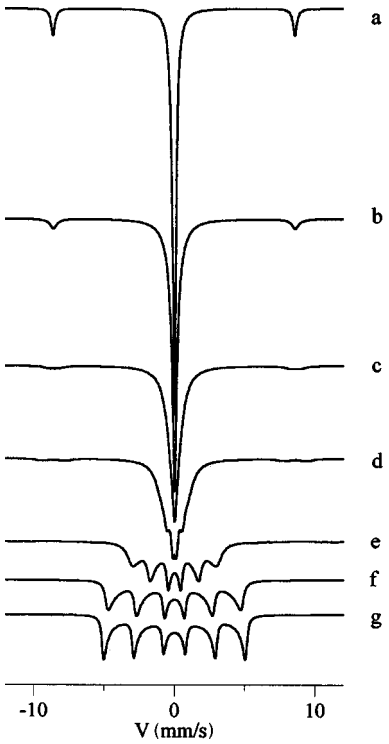

FIG. 6. Mössbauer spectra in the 100-MHz rf field of different strengths $h_0/h_{ex}=1.0$, 0.3, 0.2908, 0.2906, and 0.28, and 0.001 from (a) to (g) at $T/T_C=0.5$, $\omega_L=60$ MHz, and $p^{(0)}=200$ MHz for a uniform distribution of easiest magnetization axes of the particles.

be essentially more prolonged. As seen from Fig. 5(d), the hysteresis curves for particles with different orientations of the easiest magnetization axes strongly differ near the transition point and, correspondingly, that is true for Mössbauer spectra. Since the resulting spectrum is a superposition of partial ones for particles of different kind, the field dependence of the spectral shape is observed down to rather low rf field, which becomes apparent as remarkable line shifts and changes in shapes of particular lines.

In similar manner the calculations of Mössbauer spectra can be performed in the presence of distribution of particles over their volumes and for multiphase systems as well as for the cases when all the distributions mentioned take place. However, there are a variety of situations so that the problem needs to be specially studied, which will be done elsewhere.

VII. CONCLUSIONS

Thus, in the present study, the general equations which describe the transformation of absorption Mössbauer spectra under rf-field excitation with arbitrary rf-field frequency and strength have been derived. Within the model chosen for a ferromagnet as a system of interacting Stoner-Wohlfarth single-domain particles, the evolution of the spectra as a function of temperature and the initial relaxation parameters can be traced. It is found that the collapse effect is of a pronounced threshold character with respect to the rf-field strength and does not need strong rf fields for its realization. The effect reveals in clear form even in rf fields by far lower than the exchange and dipole-dipole fields. The necessary condition for the observation of the collapse effect is only a rf field of such a strength that the corresponding magnetization curves would be symmetrical in time reversal.

The theory developed allows the corresponding calculations for multiphase systems to be performed which, from a theoretical point of view, are also interesting by the fact that therein evidently occurs a situation when the resulting spectrum is a superposition of partial ones for particular superparamagnetic particles and the hyperfine field at nuclei does not follow the total magnetic moment of the whole sample, but the magnetic moment of a particular particle. This circumstance determines a rather nontrivial transition from the collapsed line (in a strong enough rf field) to the well-resolved hyperfine structure (in a weak rf field).

In real conditions a number of factors should be taken into account to describe the experimental data. Due to the pronounced threshold specificity of the effect near the transition field, it is necessary to take into consideration a small spread in the values of parameters such as temperature and weak constant magnetic field as well as the rf field strength, the latter inevitably arising due to the skin effect. Averaging over the distributions of the parameters is directly performed on the basis of the derived equations and offers no special complication. Besides that, the rf field may cause additional spectral lines appearing as sidebands similar to that due to magnetostriction. Within the until now existing theories, this effect only is taken into account in terms of a simple multiplication of the initial spectrum at corresponding periods (see Ref. 12). All these problems need to be studied in detail and will be considered for future work.

[1] L. Pfeiffer, J. Appl. Phys. **42**, 1725 (1971).
[2] L. Pfeiffer, in *Mössbauer Effect Methodology*, edited by I. J. Gruverman (Plenum, New York, 1972), Vol. 7, p. 263.
[3] G. Albanese and G. Asti, Nuovo Cimento B **6**, 153 (1971).
[4] M. Kopcewicz, J. Phys. (France) Colloq. **37**, C6-107 (1976).
[5] M. Kopcewicz, Phys. Status Solidi A **46**, 675 (1978).
[6] M. Kopcewicz and A. Kotlicki, J. Phys. Chem. Solids **41**, 631 (1980).
[7] M. Kopcewicz, U. Gonser, and H.-G. Wagner, Nucl. Instrum. Methods Phys. Res. **199**, 163 (1982).
[8] M. Kopcewicz, Struct. Chem. **2**, 313 (1991).
[9] T. Graf, M. Kopcewicz, and J. Hesse, Nanostruct. Mater. **6**, 937 (1995).
[10] M. Kopcewicz, J. Jagielski, T. Graf, M. Fricke, and J. Hesse, Hyperfine Interact. **94**, 2223 (1994).
[11] T. Graf, M. Kopcewicz, and J. Hesse, J. Phys. Condens. Matter **8**, 3897 (1996).
[12] N. Heiman, L. Pfeiffer, and J. C. Walker, Phys. Rev. Lett. **21**, 93 (1968).
[13] N. Heiman, J. C. Walker, and L. Pfeiffer, Phys. Rev. **184**, 281 (1969).
[14] Yu. V. Baldokhin, S. A. Borshch, L. M. Klinger, and V. A. Povitsky, Zh. Eksp. Teor. Fiz. **63**, 708 (1972) [Sov. Phys. JETP **36**, 374 (1972)].
[15] S. Olariu, I. Popesku, and C. B. Collins, Phys. Rev. C **23**, 50 (1981); **23**, 1007 (1981).

[16] S. R. Julian and J. M. Daniels, Phys. Rev. B **38**, 4394 (1988).
[17] A. Yu. Dzyublik, Phys. Status Solidi B **194**, 699 (1996).
[18] E. C. Stoner and E. P. Wohlfarth, Philos. Trans. R. Soc. London Ser. A **240**, 599 (1948).
[19] S. Morup, J. A. Dumestic, and H. Topsoe, in *Applications of Mössbauer Spectroscopy*, edited by R. L. Cohen (Academic, New York, 1980), Vol. II, p. 1.
[20] J. L. Dormann, Rev. Phys. Appl. **16**, 275 (1981).
[21] E. Tronc and J. P. Jolivet, J. Phys. (France) Colloq. **49**, C8-1823 (1988).
[22] W. Heitler, *Quantum Theory of Radiation* (Clarendon, Oxford, 1954).
[23] P. W. Anderson and P. R. Weiss, Rev. Mod. Phys. **25**, 269 (1953).
[24] P. W. Anderson, J. Phys. Soc. Jpn. **9**, 316 (1954).
[25] L. Cianchi, P. Moretti, M. Mancini, and G. Spina, Rep. Prog. Phys. **49**, 1243 (1986).
[26] K. S. Singwi and A. Sjolander, Phys. Rev. **120**, 1093 (1960).
[27] A. Aharoni, Phys. Rev. **177**, 793 (1969).